10.7 NUMERICAL SIMULATION OF A SQUALL LINE OBSERVED DURING MAP IOP 2A

Evelyne Richard [1,2], Stéphanie Cosma [3],
Pierre Tabary [4] and Martin Hagen [2]

(1) Laboratoire d'Aérologie, Toulouse, France
(2) Institut für Physik der Atmosphäre, DLR, Oberpfaffenhofen, Germany
(3) Service d'Aéronomie, Paris, France
(4) Centre d'étude des Environnements Terrestre et Planétaire, Vélizy, France

1. INTRODUCTION

During the MAP experiment (Bougeault et al., 2001), in the afternoon and evening of September 17, 1999 (MAP-IOP2a), a major squall line developed over the mountains northwest of the Lago Maggiore and moved southeastwards above the radar network allowing to collect a detailed and comprehensive data set. This event has been simulated with the non-hydrostatic MESO-NH model. In this paper the emphasis is put on the use of radar data to obtain a quantitative assessment of the model results.

2. OBSERVATIONS

For the purpose of the MAP experiment, two research radars, the French Ronsard and the American S-Pol, were installed in the vicinity of the Lago Maggiore. Their measurements complemented those of the Monte Lema Swiss operational radar. Fig. 1 presents the time evolution of the squall line as it has been observed with these three radars. Around 17 UTC, convection cells were initiated on the Alpine slopes. At 19 UTC they merged into a well defined squall line northeast southwest oriented which then propagated south-east. Later in the evening (21 UTC) further convection developed ahead of the line in response to the converging low-level flows originating on one side from the Ligurian sea and on the other side from the Adriatic sea (cf Tabary et al., in this proceeding for a more detailed description of this event).

2. NUMERICAL SETUP

The simulations were carried out with the non hydrostatic MESO-NH model (Lafore et al., 1998). The model was run over three nested domains with increasing horizontal resolutions (32km, 8km and 2km). The inner most domain is centered over the Lago Maggiore and extends over 300kmx300km. All the simulations start on September 17, 12 UTC and last till September 18, 00 UTC.

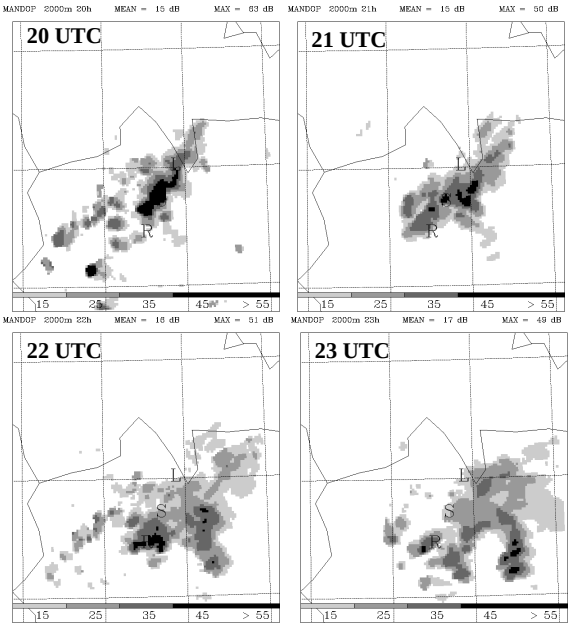

Figure 1: Time evolution of the observed reflectivity field (in dBZ) at 2000m ASL: Composite images resulting from the analysis of the Monte Lema, S-Pol, and Ronsard radar measurements. The letters L, S, and R indicate the respective locations of the threei radars. The solid lines represents the political boarders, and the parallels and meridians with a 1^o spacing.

Four experiments were performed. The control run (E1) was initialized and forced with ECMWF analysis and made use of the standard microphysical scheme of the model which includes 3 categories of ice particules (pristine ice, agregates and graupeln). The experiment E2 is identical to E1 except that the model was initialized and forced with the French ARPEGE analysis. The two other experiments aimed to study the sensitivity of the results

* *Corresponding author address*:
Evelyne Richard, Laboratoire d'Aérologie, OMP, 14 avenue E. Belin, 31650, Toulouse, France;
e-mail : rice@aero.obs-mip.fr.

to the microphysical scheme. The experiment E3 differs from E1 by the fact that only warm microphysical processes were accounted for whereas in experiment E4 the graupel characteristics have been replaced by those of denser hail particules. This later experiment was motivated by some S-Pol observations which indicates the presence of significant amount of hailstones specially in the early stage of the squall line development.

2. NUMERICAL RESULTS

Fig. 2 presents in the same format than Fig. 1 the time evolution of the computed reflectivity obtained in the control experiment. Globally the generation, propagation and life cycle of the squall line are fairly well reproduced by the simulation. The reflectivity maxima (50 to 55 dBZ) are in the same range than the measured values.

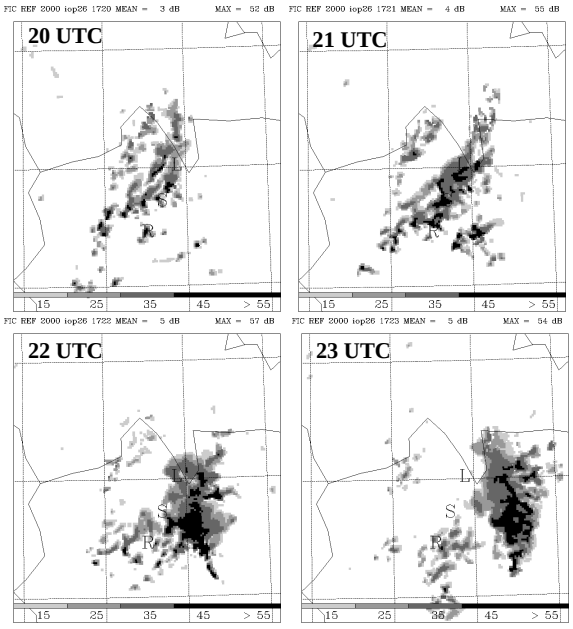

Figure 2: Time evolution of the instantaneous simulated reflectivity field at 2000m ASL. Results of the control experiment E1 initialized with ECMWF analysis.

The experiment E2 performed with the ARPEGE analysis lead to quite different results which do not fit the observations anymore. In this experiment there is very little orographic triggering from the Alpine slopes (see Fig. 3). Convection mainly develops over the plain, occurs earlier and further east that in the previous experiment. This contrasted behaviour between the two simulations appears to be mainly related to differences in the analyzed low-level wind fields, particularly noticeable over the Mediterranean See. Results from these two experiments indicate that high-resolution models could be a quite valuable tool to simulate and eventually forecast such meteorological events but only if the correct forcings are present in the analysis which provides the model initial state.

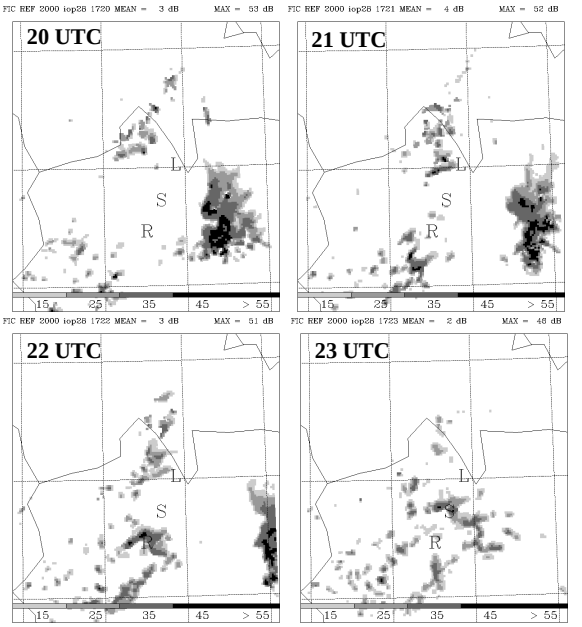

Figure 3: Time evolution of the simulated reflectivity field at 2000m ASL. Results of the experiment E2 initialized with ARPEGE analysis.

Another issue linked with high-resolution modelling deals with the complexity of the microphysical scheme. How detailed should be the representation of the different hydrometeores? How sensitive is the ground precipitation to the details of the scheme? Fig. 4 shows the accumulated precipitation field derived from radar measurements (a and b) and computed in the 4 numerical experiments (c to f). Fig 4a presents the 24h accumulated precipitation from September 17, 06 UTC to September 18, 06 UTC that can be compared with rain gauges measurements available over this time period. Comparison with Fig 4b, identical to Fig. 4a but restricted to the 12h of the simulation period, indicates that most of the rain occurred in this later time window. Comparing the different numerical fields, it is clear that as expected experiment E2 gives the worst results. It is interesting to note that experiment E3 which considers only liquid hydrometeores concentrates the precipitation over small specific areas whereas in experiments E1 and E4 the precipitation pattern extends further south east. Actually the ice particules contribute to sustain the squall line which has a longer life cycle in experiments E1 and E4 than in E3. E1 and E4 produce quite similar precipitation pattern but the precipitation amount is significantly increased when hail is present.

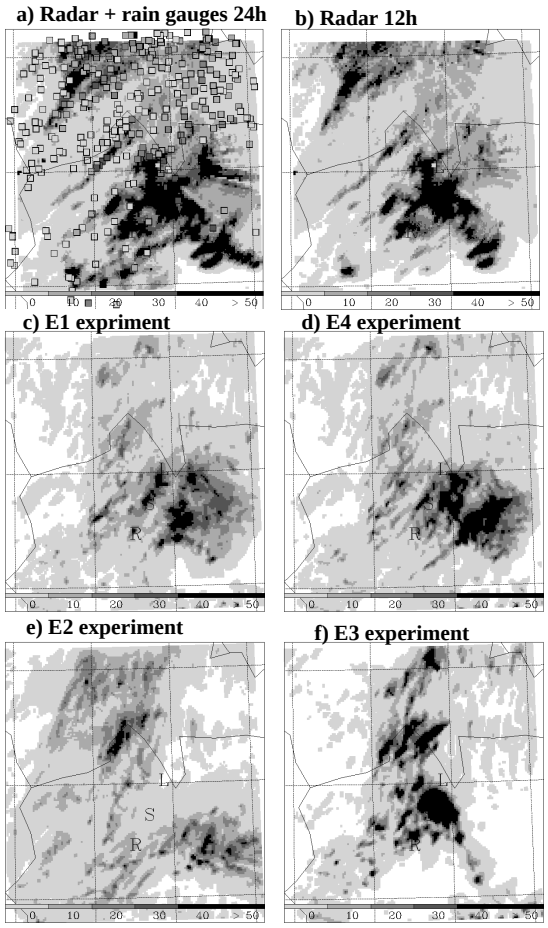

Figure 4: a) Radar derived precipitation accumulated over 24h (from Sep. 17, 06 UTC to Sept 18, 06 UTC). The squares indicate the location of the available rain gauges measurements. b) Same as a) but over 12h (from sept. 17, 12 UTC to Sept 18, 00UTC). c) d) e) and f) Computed accumulated precipitation over the same 12h for the four numerical experiments.

3. QUANTITATIVE COMPARISON

In order to get some crude but objective criteria for comparison, correlation coefficients have been computed between the radar derived fields and the surface measurements (although only very few data are available in the area of maximum precipitation, see fig. 4a). The correlation coefficient 0.68 ist not very high and shows that radar derived precipitation are still not very accurate specially over mountainous terrain. As indicated in Table 1, when the computation is restricted to the 12h time period, the correlation does not change much. The same procedure has been used to evaluate model results. With computed precipitation, the correlation coefficients significantly drop and hardly reach 0.4. But it is interesting to note that what was inferred from the time evolutions is quite well reflected in this quantative comparison. Experiments E2 (ARPEGE analysis) and E3 (warm microphysics) provide the worst results. Moreover there is a significant improvement when hail particules are substituted to graupeln particles.

Radar 24h	radar 12h	E1	E2	E3	E4
0.68	0.68	0.31	0.19	0.20	0.42

Table 1 : Correlation coefficients between the precipitation fields shown in Fig.4 and the rain gauges measurements.

A second trial of quantitative comparison has been performed using reflectivities instead of precipitation. First of all reflectivity data are direct (as opposed to derived) measurements. Then they are available in the 4D space and therefore allow to evaluate both the spatial structure and the time evolution of the precipitating system. A sample of this comparison is provided in Fig. 5 which shows the time evolution of the correlation coefficient between measured and computed reflectivities at two different altitudes (below and above the melting layer). For experiments 1 and 4 correlation coefficients are of the order of .5. Futhermore the figure confirms the better results of experiment 4 almost all along the simulation period.

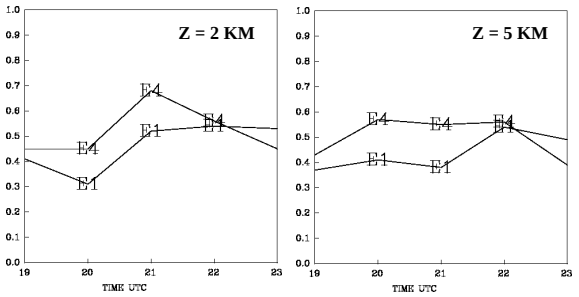

Figure 5: Time evolution of the correlation coefficients between measured and computed reflectivities for experiments 1 and 4, and at the 2 and 5 km altitudes.

4. REFERENCES

Bougeault, P., P. Binder, A. Buzzi, R. Dirks, R. Houze, J. Kuettner, R.B. Smith, R. Steinacker, H. Volkert and all the MAP scientists, 2001: The MAP special observing period. Bull. Am. Meteor. Soc, 82, 433-462.

Lafore, J. P., J. Stein, N. Asencio, P. Bougeault, V. Ducrocq, J. Duron, C. Fischer, P. Hereil, P. Mascart, J. P. Pinty, J. L. Redelsperger, E. Richard, and J. Vila-Guerau de Arellano, 1998: The Meso-NH Atmospheric Simulation System. Part I: Adiabatic formulation and control simulations. Annales Geophysicae, 16,90-109.

Tabary, P., G. Scialom, and E. le Bouar, 2001: Microphysical description of a mid-latitude squall line deduced from polarimetric measurements. This proceeding.